Solar Physics
DOI: 10.1007/•••••-•••-•••-••••-•

# Line-of-sight observables algorithms for the *Helioseismic and Magnetic Imager* (HMI) Instrument onboard the *Solar Dynamics Observatory* (SDO) tested with IBIS observations

**Sébastien Couvidat**[1] · **Sebastian P. Rajaguru**[2] · **Richard Wachter**[3] · **Kasiviswanathan Sankarasubramanian**[2] · **Jesper Schou**[1] · **Philip H. Scherrer**[1]

Received: 5 July 2011



**Abstract** The *Helioseismic and Magnetic Imager* (HMI) instrument produces line-of-sight observables (Doppler velocity, magnetic field strength, Fe I linewidth, linedepth, and continuum intensity) as well as vector-magnetic-field maps at the solar surface. The accuracy of the line-of-sight observables is contingent upon the quality of the observables algorithm used to translate HMI filtergrams of an observables sequence into observables quantities. Using one hour of high-cadence imaging spectropolarimetric observation of a sunspot in the Fe I line at 6173 Å through the *Interferometric BI-dimensional Spectrometer* (IBIS) and the Milne-Eddington inversion of the corresponding Stokes vectors, we test the accuracy of the observables algorithm currently implemented in the HMI pipeline at Stanford University: the so-called MDI-like algorithm. We also compare this algorithm to others that may be implemented in the future in an attempt at improving the accuracy of HMI observables: a least-squares fit with a Gaussian profile, a least-squares fit with a Voigt profile, and the use of second Fourier coefficients in the MDI-like algorithm.

**Keywords:** Sun: helioseismology, Instrument: SDO/HMI

## 1. Introduction

The *Helioseismic and Magnetic Imager* instrument (HMI; Schou *et al.*, 2011) onboard the *Solar Dynamics Observatory* satellite (SDO) makes measurements,

[1] W.W. Hansen Experimental Physics Laboratory
491 S Service Road, Stanford University
Stanford, CA 94305-4085, USA
email: couvidat@stanford.edu
[2] Indian Institute of Astrophysics, Bangalore, India
[3] Germany

in the absorption line Fe I centered at the in-air wavelength 6173.3433 Å (*e.g.* Norton *et al.*, 2006; Dravins, Lindegren, and Nordlund, 1981), of the motion of the solar photosphere to study solar oscillations, and of the polarization to study all three components of the photospheric magnetic field. HMI samples the neutral iron line at six positions (wavelengths) symmetrical around the line center at rest. The line-of-sight (LOS) observables are produced every 45 s and are: the Doppler velocity at the solar surface, the LOS magnetic field strength, the Fe I linewidth, the linedepth, and the continuum intensity. These observables are calculated using 12 filtergrams: images taken at 6 wavelengths and 2 polarizations (left-circular and right-circular polarizations, hereafter LCP and RCP). Unlike the Michelson Doppler Imager (MDI) instrument on which HMI is based, the observables calculations are performed on the ground at Stanford University, and not on board the spacecraft. This allows for more flexibility regarding which observables algorithm to apply, and makes reprocessing of these observables possible in the eventuality that a better algorithm is later implemented. On June 8, 2007, the sunspot NOAA AR10960 was observed by the Interferometric BI-dimensional Spectrometer (IBIS; Cavallini 2006) instrument installed at the Dunn Solar Telescope of the National Solar Observatory in Sacramento Peak (New Mexico, USA). The full Stokes profile (I,Q,U, and V) of the Fe I line was scanned and imaged for 7 h at a cadence of 47.5 s, close to the HMI cadence (see Rajaguru et *al.*, 2010, for details on these IBIS data processing and calibration). These IBIS images have a spectral and spatial resolutions of 25 mÅ and 0.165" respectively (*i.e.* a spatial resolution three times better than HMI), and the Fe I line was sampled at 23 different wavelengths. We select a 1 hour-long observation (the first hour) out of the 7 observation hours, to keep only the best seeing interval and to match the time interval selected for the Milne-Eddington inversion of the Stokes vectors (Skumanich and Lites, 1987).

The IBIS observations present some advantages over the HMI ones because the iron line is scanned at 23 wavelengths instead of 6. This allows for an interpolation of the line profiles at each pixel on a finer wavelength grid: we can therefore simulate HMI observations by applying the filter transmission profiles to these interpolated Fe I lines, and test the accuracy of not only Doppler velocity and magnetic-field strength but also the linewidth, linedepth, and continuum intensity returned by the MDI-like algorithm. We can also test other observables algorithms, like a least-squares fit with an appropriate Fe I profile. Moreover the Sun-Earth radial velocity varied little during the IBIS observation timespan (from $-120.98$ m s$^{-1}$ to $-95.43$ m s$^{-1}$ during the 1h-long interval, compared to a 358 m s$^{-1}$ change for the HMI-Sun radial velocity over the same timespan on June 8, 2011). Another consideration for using IBIS data and their Milne-Eddington inversion is that, at the time of writing, the full Stokes-vector inversion data of HMI have not yet been officially released: the code vfisv (Borrero *et al.*, 2010) is being fine-tuned. However, the spatial resolution of IBIS is different from HMI, a fact that needs to be factored in when analysing the IBIS results: because, among others, of convective blueshift (depending on how well granules are resolved), a different spatial resolution translates into a different Fe I line profile. In Section 2 we describe the MDI-like algorithm currently implemented in the HMI pipeline, in Section 3 we describe other observables

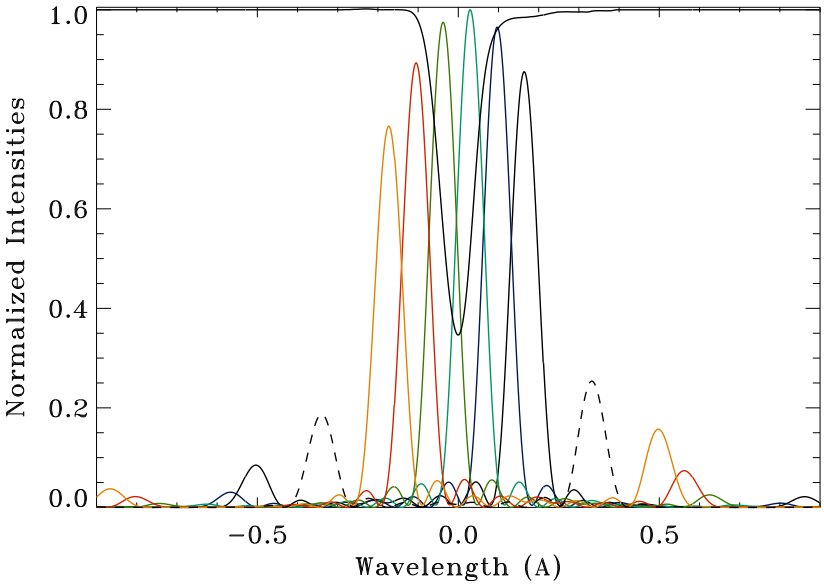


**Figure 1.** Example of HMI sampling-position profiles obtained from calibration procedures. Six tuning positions are shown here with respect to the Fe I solar line (black line) at disk center and at rest, on top of the continuum tuning position (dashed line). The continuum tuning position can be used to estimate the solar continuum intensity. The Fe I line profile was provided by R. K. Ulrich and obtained at the Mount Wilson Observatory.

algorithms tested, and in Section 4 we introduce the IBIS data used. We present the results in Section 5 and we conclude in Section 6.

## 2. MDI-like Algorithm

The MDI-like algorithm is based on what was implemented for the SOHO/MDI instrument (Scherrer et *al.*, 1995). It combines filtergrams taken at 6 wavelengths. The actual profiles of the corresponding 6 filter transmittances need to be accurately known. The HMI optical-filter system is composed of a front window, a blocking filter, a five-stage Lyot filter, and two Michelson interferometers. The Lyot element E1 (the element with the lowest FWHM) and the two Michelson interferometers are tunable and allow for the taking of the filtergrams at 6 different wavelengths. The calculation of the resulting filter transmission profiles is detailed in Couvidat et *al.* (2011). An example of such profiles is reproduced on Figure 1. These profiles slowly change with time and vary across the HMI CCDs.

The MDI-like algorithm starts with a discrete estimate of the first and second Fourier coefficients $a_n$ and $b_n$ of the Fe I line profile $I(\lambda)$ (where $\lambda$ is the

wavelength):

$$a_1 = \frac{2}{T}\int_{-\frac{T}{2}}^{+\frac{T}{2}} I(\lambda)\cos\left(2\pi\frac{\lambda}{T}\right)d\lambda \ ; \ b_1 = \frac{2}{T}\int_{-\frac{T}{2}}^{+\frac{T}{2}} I(\lambda)\sin\left(2\pi\frac{\lambda}{T}\right)d\lambda \quad (1)$$

$$a_2 = \frac{2}{T}\int_{-\frac{T}{2}}^{+\frac{T}{2}} I(\lambda)\cos\left(4\pi\frac{\lambda}{T}\right)d\lambda \ ; \ b_2 = \frac{2}{T}\int_{-\frac{T}{2}}^{+\frac{T}{2}} I(\lambda)\sin\left(4\pi\frac{\lambda}{T}\right)d\lambda \quad (2)$$

where $T$ is the "period" of the line profile, taken to be the FWHM of the tunable Lyot element E1 (nominally 344 mÅ). Assuming that the solar line has a Gaussian profile:

$$I(\lambda) = I_c - I_d \exp\left[-\frac{(\lambda-\lambda_0)^2}{\sigma^2}\right] \quad (3)$$

where $I_c$ is the continuum intensity, $I_d$ is the linedepth, $\lambda_0$ is the Doppler shift, and $\sigma$ is related to the linewidth, the Doppler velocity $v$ can be expressed as:

$$v = \frac{dv}{d\lambda}\frac{T}{2\pi}\,\mathrm{atan}\left(\frac{b_1}{a_1}\right) \quad (4)$$

with $dv/d\lambda = 299792458.0/6173.3433 = 48562.4$ m/s/Å. The second Fourier coefficients could also be used:

$$v_2 = \frac{dv}{d\lambda}\frac{T}{4\pi}\,\mathrm{atan}\left(\frac{b_2}{a_2}\right) \quad (5)$$

The linedepth $I_d$ is equal to:

$$I_d = \frac{T}{2\sigma\sqrt{\pi}}\sqrt{a_1^2+b_1^2}\exp\left(\frac{\pi^2\sigma^2}{T^2}\right) \quad (6)$$

while $\sigma$ is equal to:

$$\sigma = \frac{T}{\pi\sqrt{6}}\sqrt{\mathrm{alog}\left(\frac{a_1^2+b_1^2}{a_2^2+b_2^2}\right)} \quad (7)$$

If the linewidth $L_w$ of the Fe I line is defined as its FWHM, then $L_w = 2\sqrt{\ln(2)}\sigma$.

HMI samples the Fe line at only 6 points and the Fourier coefficients are therefore approximated as sums, for instance:

$$a_1 \approx \frac{2}{5}\sum_{j=0}^{5} I_j \cos\left(2\pi\frac{2.5-j}{6}\right) \quad (8)$$

The MDI-like algorithm calculates these $a_n$ and $b_n$ values separately for the LCP and RCP polarizations. Applying Equation (4) to the estimates of the first Fourier coefficients, two estimates of the Doppler velocity are obtained: $v_{\mathrm{LCP}}$ and $v_{\mathrm{RCP}}$ (for, respectively, LCP and RCP).

However the HMI filter transmission profiles are not delta functions, the discrete approximations to the Fourier coefficients are not perfect because of a reduced number of sampling points, and the Fe I line does not have a Gaussian profile. Therefore, the Doppler velocities $v_{\rm LCP}$ and $v_{\rm RCP}$ need to be corrected. To this end we use look-up tables obtained from a realistic model of the Fe I line profile at rest. This profile is shifted in wavelength to simulate a given Doppler velocity. At each shift, the line profile is multiplied by the 6 filter transmission profiles, and the corresponding integral values are calculated. The MDI-like algorithm is then applied. Therefore, the Doppler velocity returned by the algorithm is a function of the actual (input) Doppler velocity. The inverse function is called look-up table (table is a misnomer and is a legacy of the MDI implementation). Because the filter transmission profiles vary across the HMI CCDs, look-up tables also vary with the CCD pixel location. The tables are linearly interpolated at $v_{\rm LCP}$ and $v_{\rm RCP}$, producing the corrected Doppler velocities $V_{\rm LCP}$ and $V_{\rm RCP}$. In the rest of this paper, we call 1st Fourier-coefficient MDI-like algorithm the use of the 1st Fourier coefficients to estimate the Doppler velocities, and their subsequent correction with look-up tables.

Unfortunately, the calibration of the HMI filter profiles shows some residual errors (at the percent level) on the transmittances. Therefore, the look-up tables are imperfect. The SDO orbital velocity is known very accurately, and it is possible to use it to, partly, improve the tables. This additional step is implemented in the LOS observables code of the HMI pipeline, but will be ignored in this article.

Finally, the $V_{\rm LCP}$ and $V_{\rm RCP}$ velocities are combined to produce a Doppler-velocity estimate:

$$V = \frac{V_{\rm LCP} + V_{\rm RCP}}{2} \tag{9}$$

while the LOS magnetic field strength $B$ is:

$$B = (V_{\rm LCP} - V_{\rm RCP})K_m \tag{10}$$

Where $K_m = 1.0/(2.0 \times 4.67 \cdot 10^{-5} \times 0.000061733433 \times 2.5 \times 299792458.0)$ for a Lande g-factor of 2.5 (Norton *et al.*, 2006).

An estimate of the continuum intensity $I_c$ is obtained by "reconstructing" the solar line from the Doppler-shift estimate, linewidth, and linedepth:

$$I_c = \frac{1}{6}\sum_{j=0}^{5}\left[I_j + I_d \exp\left(-\frac{(\lambda - \lambda_0)^2}{\sigma^2}\right)\right] \tag{11}$$

where $\lambda_0$, $I_d$, and $\sigma$ are the values retrieved by Eqs (4), (6), and (7).

## 3. Other Observables Algorithms Tested

Observables algorithms other than the MDI-like algorithm based on 1st Fourier coefficients are also applied to the 1-hour averaged and wavelength-interpolated

LCP and RCP IBIS line profiles (see next section): the MDI-like algorithm with the 2nd Fourier coefficients, a least-squares fit with a Gaussian-line profile, and a least-squares fit with a Voigt profile.

Before the launch of SDO it was planned to use both the first and second Fourier coefficients when computing all the HMI LOS observables. The second Fourier coefficients are already used by the MDI-like algorithm to derive the linewidth, linedepth, and continuum intensity, but not for the Doppler velocity and magnetic field. Unfortunately, using the second Fourier coefficients turned out to be more difficult than anticipated (in particular there was a significant number of saturated pixels where the magnetic field was large, and the 2nd Fourier-coefficient velocities differed significantly from the 1st Fourier-coefficient ones). Because of tight time constraints it was decided to postpone the implementation of the second Fourier-coefficients algorithm. The result is that currently only half the information available is used, and therefore the rms variation on the Doppler velocity due to photon noise is $\sqrt{2}$ larger than it could be. A possible improvement to the current implementation of the MDI-like algorithm would be to include these second Fourier coefficients: the impact of such an inclusion is discussed here.

The MDI-like algorithm (with 1st and/or 2nd Fourier coefficients) is computationally very fast: there is no fit involved, only a combination of 6 wavelengths followed by a linear interpolation. That is a reason why this algorithm was preferred over least-squares fits. However, because the look-up tables are computed for a reference Fe I line profile obtained in the quiet Sun, the algorithm is expected to fare poorly in regions of strong magnetic field. Conversely, a least-squares fit with a reasonable model of the Fe I line profile is expected to provide more accurate results, because this line profile is adjusted during the fit to reflect the presence of magnetic fields. The simplest model of Fe I line used here is a Gaussian profile. This profile results from Doppler broadening alone, and as such is a poor approximation to the actual iron line (which also displays a significant asymmetry). A more elaborate model is the Voigt profile: a convolution between a Gaussian profile (thermal broadening) and a Lorentzian profile (produced by radiative and collisional broadenings). It is more representative of the actual Fe I line profile than a Gaussian, even though it is still symmetrical around the central wavelength at rest. For convenience, and to speed up the computations, an analytical expression to the Voigt-Hjerting function was used (Tepper Garcia, 2006):

$$I(x) = I_c - I_d \, \mathrm{e}^{-x^2} \left[ 1 - \frac{a}{\sqrt{\pi} x^2} \left( (4x^2+3)(x^2+1) \, \mathrm{e}^{-x^2} - \frac{(2x^2+3)}{x^2} \sinh(x^2) \right) \right] \tag{12}$$

Where $x = (\lambda - \lambda_0)/\sigma$, $\lambda_0$ is the Doppler shift, $\sigma$ is the linewidth of the Gaussian part of the Voigt profile, $I_c$ is the continuum intensity, and $I_d$ is related to (but is not equal to) the linedepth. This expression is an approximation to the first order in $a$, the so-called damping parameter, and is strictly valid for $a << 1$. Least-squares fits of two observed Fe I line profiles (one from the Kitt-Peak Atlas, one provided by R. Ulrich from Mount Wilson observatory and at

solar disk center) return a value for $a$ in the range $0.2 - 0.25$. This is close to the $a = 0.23$ quoted by Bell and Meltzer (1959). Here we set $a = 0.225$ (other values were tested for comparison). It can be argued that such a large $a$ value might produce a non-negligible error when using the anaytical expression of Tepper Garcia (2006).

## 4. IBIS Data

Rajaguru *et al.* (2010) describe with further details the IBIS data and their Milne-Eddington inversion utilized here. We select the first hour of data, corresponding to the best seeing interval. The format of the initial datacube is $512 \times 512 \times 23 \times 4 \times 79$, where the first two dimensions refer to the Cartesian coordinates at the solar surface (the original $1024 \times 1024$ IBIS data have been rebinned by a factor 2), the next dimensions are the number of wavelength samples (23) and of Stokes parameters (4), and the last dimension is the number of time steps (this datacube covers 1.03 hours at a cadence of 47.5 s). To compare the LOS magnetic field strength returned by the observables algorithms with the result of the Milne-Eddington (M-E) inversion of the Stokes vector, we further process the IBIS data: we select a $341 \times 341$ pixel region centered on the sunspot (same region as in Rajaguru *et al.*, 2010), and we temporally average the datacube over the full hour. Moreover, we only consider the LCP (I+V) and RCP (I-V) polarizations. Therefore the processed datacube has $341 \times 341 \times 23 \times 2$ points. At each pixel, we apply a cubic spline interpolation (and also a quadratic interpolation for comparison) of the 23-wavelength samples, to obtain the Stokes components LCP and RCP on a finer wavelength grid (with a sampling rate of 0.5 mÅ). Figure 2 shows maps of the LOS magnetic field strength (obtained with the 1st Fourier-coefficients MDI-like algorithm) and the continuum intensity of the processed IBIS data. The square window centered on the sunspot shows the area that is selected for the scatter plots of Section 5: outside this window the M-E inversion is very noisy due to low polarization signal. It is noteworthy that no attempt was made to correct for scattered light on IBIS data: therefore, the signal in the sunspot umbra partly comes, probably to a significant level, from adjacent areas and especially the penumbra.

## 5. Results

We test the accuracy of 4 observables algorithms previously described. To simulate the 12 HMI filtergrams needed to derive LOS observables, we use a set of HMI filter transmission profiles obtained from calibration procedures and valid at solar disk center. We multiply the wavelength-interpolated LCP and RCP Fe I IBIS 1 hour-averaged profiles by these filter profiles, and we compute the integral values: those are simulated HMI intensities.

To obtain the look-up tables required by the MDI-like algorithm, a reference Fe I line profile is needed. This reference profile must be the profile at rest as seen by IBIS: therefore we select a wavelength-interpolated Stokes I profile for

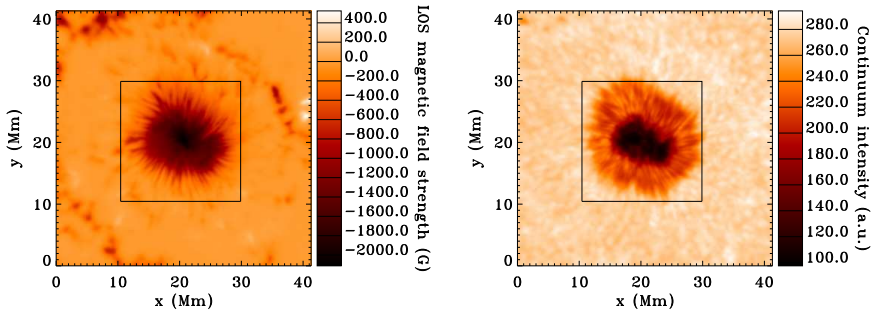


**Figure 2.** Maps of the LOS magnetic field strength (obtained with the MDI-like algorithm based on the 1st Fourier coefficients) and of the continuum intensity of the active region NOAA AR10960 of June 8, 2007, observed by the IBIS instrument. The square window centered on the sunspot shows which pixels were selected for the scatter plots of Section 5.

which the I+V and I-V components superimpose (denoting the absence of any significant magnetic field). The resulting reference line is shown on Figure 3. The magnetic field strength is close to zero at several locations in the IBIS field of view, also several reference profiles were tested: despite minor differences between these profiles, the conclusions of this article are unaffected by the choice of a specific one. It is noteworthy that the reference Fe I line profile from IBIS data is broader (with a FWHM of 131.5 mÅ instead of the 102 mÅ) and shallower (linedepth of 0.447 instead of 0.66) than reported by Norton *et al.* (2006): the difference comes from the absence of deconvolution of the IBIS line by the instrumental transmittance (the IBIS filter profiles have a FWHM of about 25 mÅ); what we refer to as the Fe I line profile is the actual profile convolved by the IBIS filter transmittance.

Figure 4 shows a cut in the Doppler velocity and LOS magnetic field strength returned by the different observables algorithms. The cut is at the latitude crossing the center of the sunspot. The average Doppler velocity in the quiet Sun returned by each algorithm has been subtracted to make comparisons easier. On this figure, the curve referenced to as "line core" shows the Doppler velocity obtained by locating the minimum of the interpolated Fe I line profiles: once the approximate location is known, a second-order polynomial fit in the wavelength range [-25,+25] mÅ around this approximate minimum is performed to determine the exact minimum. We do not expect the Doppler velocity returned by this line-core algorithm to match the results of the other observables algorithms, because, *e.g.*, Fleck, Couvidat, and Strauss (2011) showed that the MDI-like algorithm does not track the Doppler shift of the core of the line, but rather of the center of gravity of the line. Other algorithms are expected to be sensitive to different parts of the Fe I line. Also, Table 1 lists the linear (Pearson) correlation coefficients between the Doppler velocities returned by the 4 algorithms and the line-core method: correlation coefficients seem more interesting than a pixel-to-pixel comparison. The lowest correlation is obtained for the MDI-like algorithm with 2nd Fourier coefficients. Table 2 lists the correlation coefficients

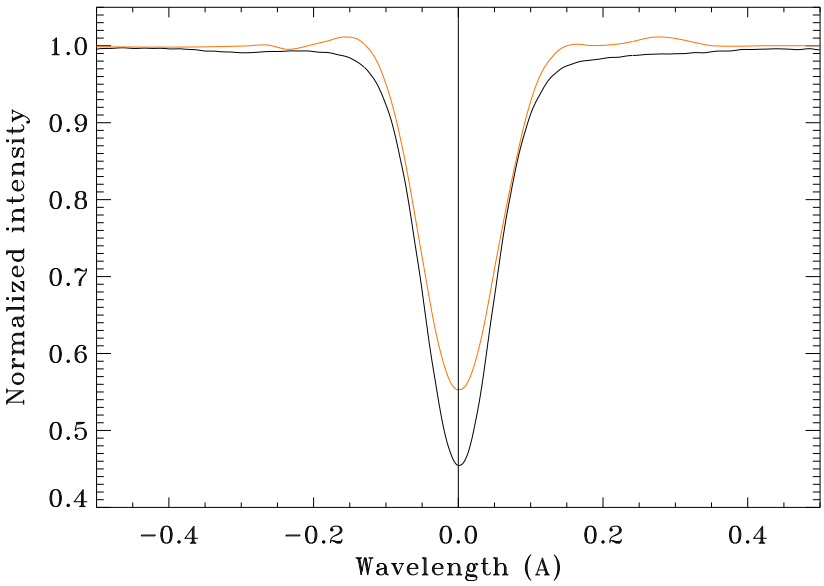


**Figure 3.** Comparison of Fe I line profiles: the black solid line is the profile from the Kitt Peak atlas obtained by the Kitt Peak-McMath Pierce telescope while the solid orange line is the reference Fe I line profile used here to calculate the look-up tables for the MDI-like algorithm and obtained from the hour-long averaging of IBIS data.

**Table 1.** Pearson linear correlation coefficients between the LOS Doppler velocities returned by different algorithms for the pixels located in the square window of Figure 2.

| | 1st Fourier | 2nd Fourier | Gauss | Voigt |
|---|---|---|---|---|
| line core | 80.7 | 24.5 | 76.9 | 76.9 |
| 1st Fourier | 100.0 | 40.0 | 98.7 | 98.7 |

for the LOS magnetic field strength. In this table and in the rest of this paper, M-E LOS inversion (or M-E LOS magnetic field) refers to the magnetic field strength inverted by the Milne-Eddington code and multiplied by the cosine of the inclination angle. Similarly to the Doppler velocity, the lowest correlation is obtained for the 2nd Fourier-coefficients MDI-like algorithm, even though the difference in correlation coefficients between algorithms is not as large for the magnetic field.

Figure 4 shows that the 2nd Fourier-coefficient MDI-like algorithm fares rather poorly in the sunspot, compared to the other algorithms tested. In the sunspot penumbra, the Doppler velocity returned by the 2nd Fourier coefficients is strikingly different from the velocity returned by the 1st Fourier coefficients (and also the least-squares fits), as is also evidenced by the low correlation

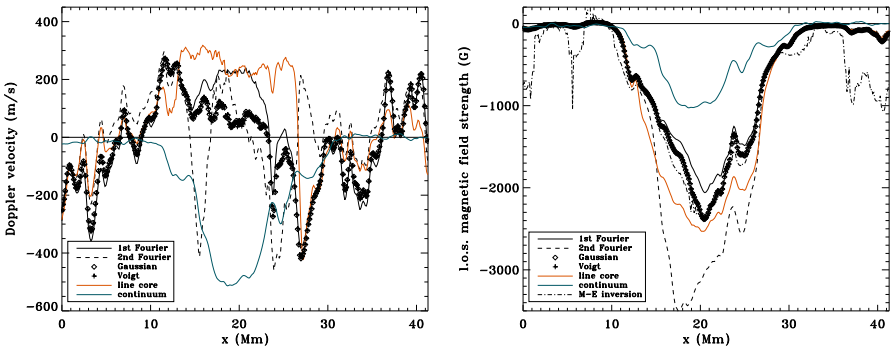


**Figure 4.** LOS Doppler velocities and magnetic field strengths returned by various observables algorithms. This is a cut at the latitude crossing the center of the sunspot. The blue curve labeled "continuum" shows a normalized continuum intensity, for comparison.

**Table 2.** Pearson linear correlation coefficients between the LOS magnetic field strengths returned by different algorithms for the pixels located in the square window of Figure 2.

| | 1st Fourier | 2nd Fourier | Gauss | Voigt |
|---|---|---|---|---|
| M-E inversion | 95.3 | 94.7 | 95.8 | 95.8 |
| 1st Fourier | 100.0 | 96.5 | 99.8 | 99.8 |

coefficient. This is further confirmed by Figure 5, and the following scatter plots 6 to 12. In the sunspot umbra, the LOS magnetic field strength returned by the 2nd Fourier coefficient is very different from the other algorithms.

Indeed, the 2nd Fourier coefficients are very sensitive to the Fe I line shape, much more so than the 1st Fourier coefficients. The deformation affecting the I+V and I-V components in presence of a strong and inclined magnetic field is

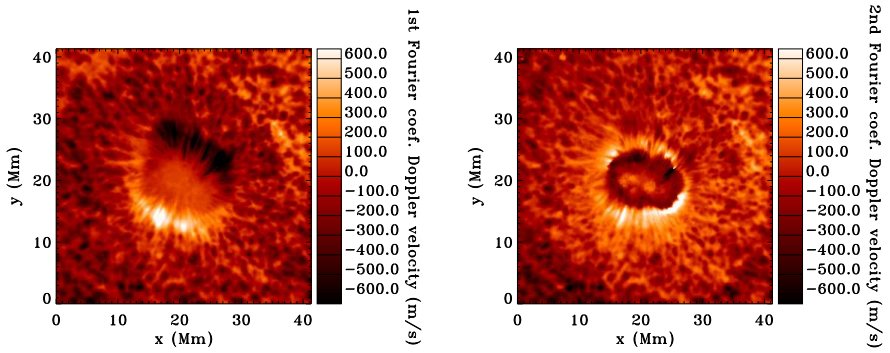


**Figure 5.** LOS Doppler velocities returned by the MDI-like algorithm using the 1st (left panel) or 2nd (right panel) Fourier coefficients.

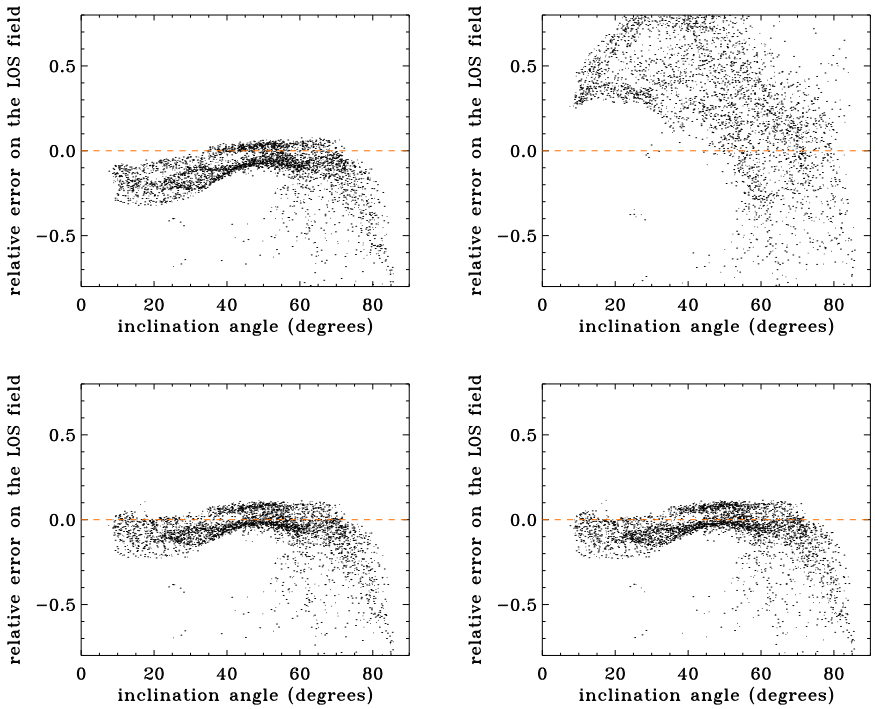


**Figure 6.** Relative errors on the LOS magnetic field strength returned by the observables algorithms with the LOS field strength returned by the M-E inversion. Upper left panel: MDI-like algorithm with 1st Fourier coefficients; Upper right panel: MDI-like algorithm with 2nd Fourier coefficients; Lower left panel: least-squares fit with a Gaussian profile; Lower right panel: least-squares fit with a Voigt profile.

not reflected in the look-up tables, thus producing large errors for the second Fourier coefficients, and explaining the difficulties encountered during the commissioning phase of SDO when trying to use these coefficients. Other algorithms (1st Fourier-coefficient MDI-like algorithm and least-squares fits) seem more robust in presence of a strong and inclined field.

The impact of a magnetic field can be further assessed. Figure 6 shows the impact of the inclination angle (relative to the vertical direction) of the field determined by the M-E inversion on the relative error in LOS field strength made by each algorithm: for the 1st Fourier-coefficient MDI-like algorithm and the least-squares fits, the error increases (in absolute value) when the inclination angle increases (for angles larger than about $50 - 60$ degrees corresponding to the penumbra). To obtain this plot only the pixels for which the absolute value of the field strength is larger than 150 Gauss and that are located inside the window shown on Figure 2 were kept, thus avoiding the noisiest values. The low inclination angles correspond to umbral signal (partly contaminated by penumbral signal due to scattering). None of the observables algorithm seems to show any dependence to the azimuth angle of the magnetic field. Figure 7 shows the impact of the inclination angle on the difference in Doppler velocity

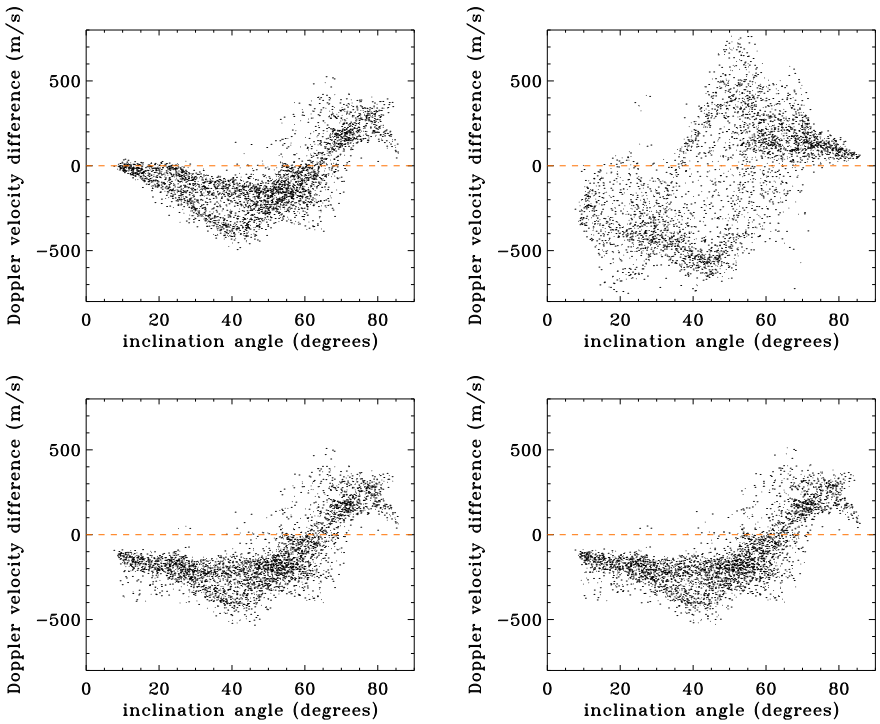


**Figure 7.** Absolute differences in the Doppler velocity returned by the observables algorithms with the velocity returned by the line-core algorithm. Upper left panel: MDI-like algorithm with 1st Fourier coefficients; Upper right panel: MDI-like algorithm with 2nd Fourier coefficients; Lower left panel: least-squares fit with a Gaussian profile; Lower right panel: least-squares fit with a Voigt profile.

(difference with the velocity returned by the line-core algorithm). Again, the absolute value of this difference does not matter much as different algorithms are sensitive to different heights in the solar atmosphere: what matters is how this difference is affected by the inclination angle. The 1st Fourier-coefficients MDI-like algorithm and the least-squares fit behave in a similar fashion: the difference in velocity is relatively stable for inclination angles smaller than about $50-60$ degrees, and then changes rapidly. The least-squares algorithms are more stable at low inclination angles than the MDI-like algorithm with 1st Fourier coefficients. The MDI-like algorithm with 2nd Fourier coefficients behaves differently and in a seemingly more random way. On Figure 8 the field stengths smaller than 1250 G (black dots) were isolated from stronger fields (orange dots). These Doppler velocity scatter plots show 2 branches (one orange, one black): the relation between the velocity returned by the algorithms tested here and the line-core algorithm clearly depends on the magnetic field strength. As previously observed, the 1st Fourier-coefficient MDI-like, Gaussian least-squares, and Voigt least-squares algorithms behave very similarly, unlike the 2nd Fourier-coefficient MDI-like algorithm which returns spurious velocities in regions of strong magnetic fields. Indeed, the orange branch of the upper right panel of

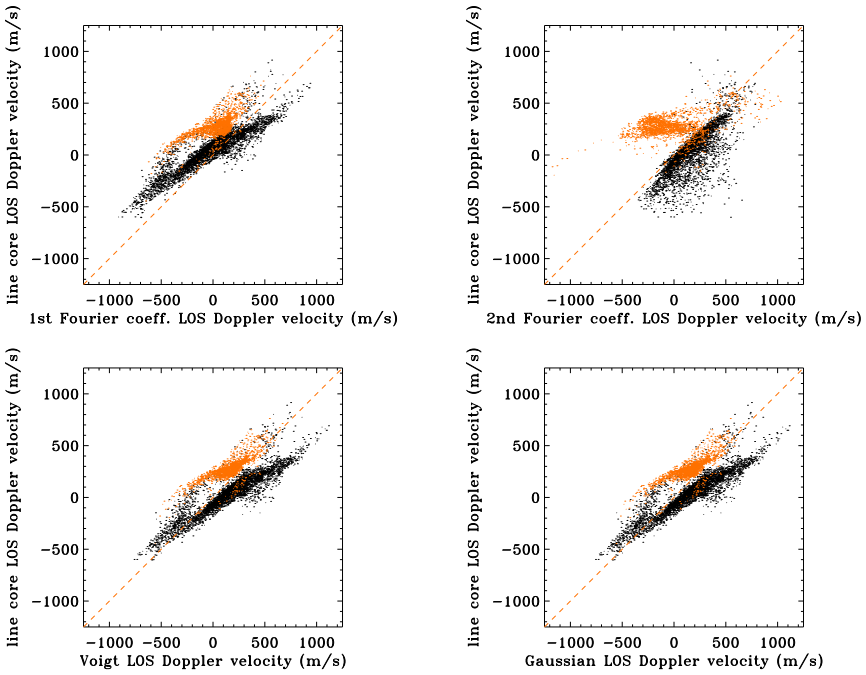


**Figure 8.** Scatter plots of the Doppler velocities returned by different algorithms with the velocity returned by the line-core algorithm. Upper left panel: the 1st Fourier-coefficient MDI–like algorithm; upper right panel: 2nd Fourier-coefficient MDI-like algorithm; lower left panel: least-squares fit with a Voigt profile; lower right panel: least-squares fit with a Gaussian profile. Black dots: magnetic field strength $< 1250$ G; orange dots: magnetic field strength $> 1250$ G.

Figure 8 is almost horizontal, and differs greatly from the black branch. Another reason (on top of the deformation of the Fe I line resulting from strong and inclined fields) why the two branches differ in all these panels might be that the geometric height in the atmosphere where the Doppler signal is formed is not the same above the quiet Sun and above a sunspot. It must be mentioned that even though we presented separately the impact of field strength and field inclination, the two effects are actually not readily disentangled with the set of data used because there is a strong relationship between the two: strong fields — located in the umbra — have small inclinations, while weak fields — in the penumbra — have large inclinations.

Overall, as can be seen on Figures 4, 6, 7, 8, and 9, least-squares fits seem to perform better than the 1st Fourier-coefficient MDI-like algorithm in presence of a magnetic field, while the 2nd Fourier-coefficient MDI-like algorithm appears to be the least accurate algorithm. The idea of averaging Doppler velocities and magnetic-field strength obtained from the 1st and 2nd Fourier coefficients might not be beneficial to these observables: it will reduce the noise level due to photon noise and might improve the observables determination in the quiet Sun, but it will make things worse in presence of strong magnetic fields.

The 1st Fourier-coefficient MDI-like algorithm underestimates (in absolute value) the LOS magnetic field strength inside a sunspot by up to 30% in the

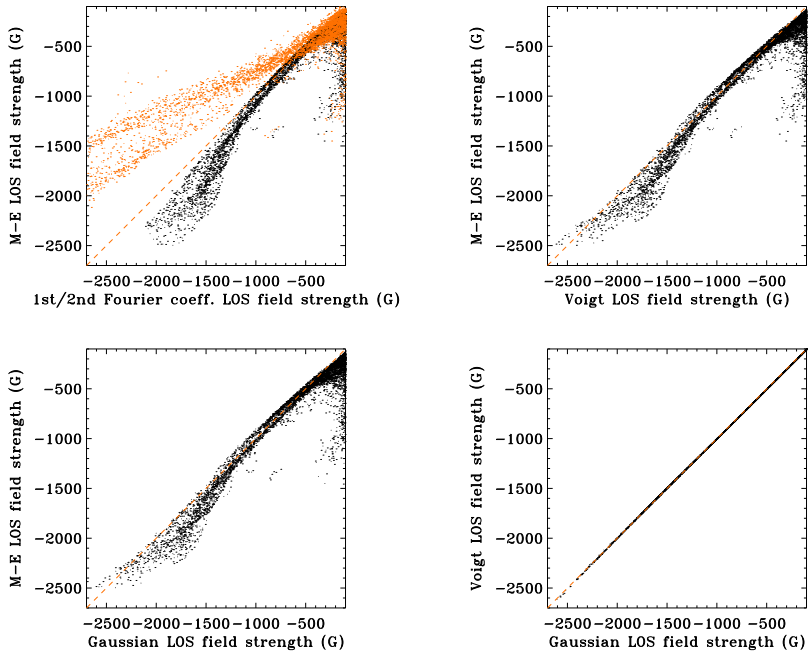


**Figure 9.** Scatter plots of the LOS magnetic-field strengths returned by different algorithms with the LOS field strength returned by the M-E inversion. Upper left panel: the 1st (in black) and 2nd (in orange) Fourier-coefficient MDI-like algorithm; upper right panel: least-squares fit with a Voigt profile; lower left panel: least-squares fit with a Gaussian profile; lower right panel: comparison between least-squares fit with a Voigt and Gaussian profile.

umbra (with an average value of $\approx$ 20%). On the contrary, the 2nd Fourier-coefficients MDI-like algorithm overestimates this field strength by up to 50%. The least-squares fit with a Gaussian or Voigt profile provides more accurate results, but still slightly underestimates the actual LOS field strength in the sunspot umbra (by $\approx$ 10% on average). A problem with least-squares fits is that there are a few pixels — mainly in the sunspot umbra — for which the gradient-expansion algorithm used did not converge: this issue does not arise with MDI-like algorithms which always return a value. Overall the use of a Voigt profile does not seem to improve the determination of the LOS observables significantly more than what a simpler Gaussian profile does (see Figures 8 and 9: the Voigt and Gaussian profiles return very similar values). The use of a Voigt profile with the analytical expression (4) actually makes linedepth and linewidth more difficult to determine than with a basic Gaussian profile, because these quantities do not appear explicitely in the equation and must be derived from the fitted quantities $I_d$ and $\sigma$ (the relation depends on the damping parameter $a$).

### 5.1. Other observables quantities: linewidth, linedepth, and continuum intensity

An advantage of using IBIS data sampled at 23 different wavelengths is that after interpolation we can also test how linewidth, linedepth, and continuum intensity returned by the observables algorithms compare to the actual ones. Figure 10 shows the linewidth returned by the different algorithms, while Figure 11 shows the linedepth, and Figure 12 shows the continuum intensity. On these three figures, we separated the pixels with an inclination of the magnetic field lower than 57° (the median inclination) from the pixels with a more inclined field on the left panels, and we separated the pixels with a field strength lower than 1250 G (in absolute value) from those with a stronger field on the right panels. The measured values (FWHMs, linedepths, and continuum intensities) are those directly measured on the interpolated IBIS profiles: we measured separately the LCP and RCP components, and averaged the result. For the 4 algorithms the dispersion of results seems to increase with the magnetic field strength while the possible impact of inclined magnetic fields is more difficult to interpret, except for the linewidth determined with the MDI-like algorithm: in this case, it appears that the scatter plot is closer to a linear relation for less inclined fields. The MDI-like algorithm (using both 1st and 2nd Fourier coefficients for these quantities) fares relatively poorly in presence of a magnetic field: it significantly underestimates the linewidth in the sunspot umbra and penumbra (by up to $\approx 15\%$). This is not surprising, as the presence of an inclined field distorts the Fe I line profile (with Zeeman splitting the $\sigma$ components of a longitudinal field are contaminated by the $\pi$ component when the inclination is different from 0): this profile is significantly different from the profile at rest used to generate the look-up tables. The MDI-like algorithm also underestimates by a few percents the actual linewidth in the quiet Sun, probably because even in the quiet Sun the Fe I line is not a Gaussian profile and is asymmetrical. It might be useful to produce look-up tables to correct the linewidth and linedepth, similarly to what is done for the Doppler velocity. The least-squares fits provide more robust linewidth and linedepth, even though their scatter plots also deviate from a linear relation in the sunspot. The linedepth returned by the MDI-like algorithm shows a large dispersion relative to least-squares fits: for instance, for a measured linedepth of 0.45, the MDI-like algorithm returns linedepths ranging from 0.42 to more than 0.6, depending on magnetic field strength and inclination.

The continuum intensity returned by the MDI-like algorithm displays a seemingly bizarre behaviour: it first deviates from a linear relation as the normalized continuum intensity decreases from 1 to about 0.5 or so (it underestimates the actual intensity), and then exhibits a linear behaviour for lower intensities. Least-squares algorithms slightly overestimate the actual continuum intensity in a sunspot.

## 6. Conclusion

This article uses spectropolarimetric images of the solar surface obtained by the IBIS instrument to test the precision of the LOS observables returned by the

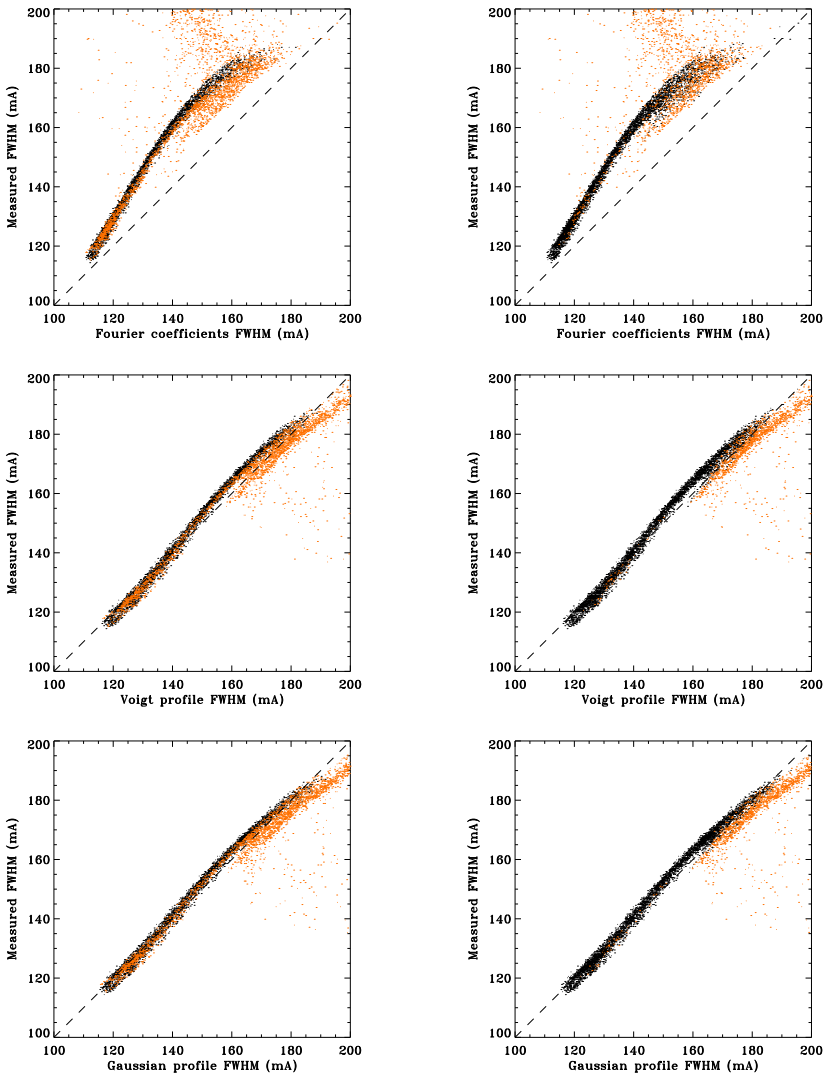


**Figure 10.** Scatter plots of the linewidths returned by different algorithms with the actual (measured) FWHMs. Upper panels: MDI-like algorithm; middle panels: least-squares fit with a Voigt profile; lower panels: least-squares fit with a Gaussian profile. Left panels: the black dots show pixels for which the magnetic field inclination is larger than 57°, while the orange dots are for less inclined fields; right panels: the black dots show pixels for which the magnetic field strength is $< 1250$ G, while orange dots are for stronger fields.

MDI-like algorithm currently implemented in the processing pipeline of the HMI instrument at Stanford University. Three other observables algorithms were also tested: the MDI-like algorithm based on the 2nd Fourier coefficients, a least-squares fit with a Gaussian profile, and a least-squares fit with a Voigt profile. It appears that, in presence of magnetic field, the least-squares fits are more accurate than the MDI-like algorithm (as expected). The 2nd Fourier-coefficient

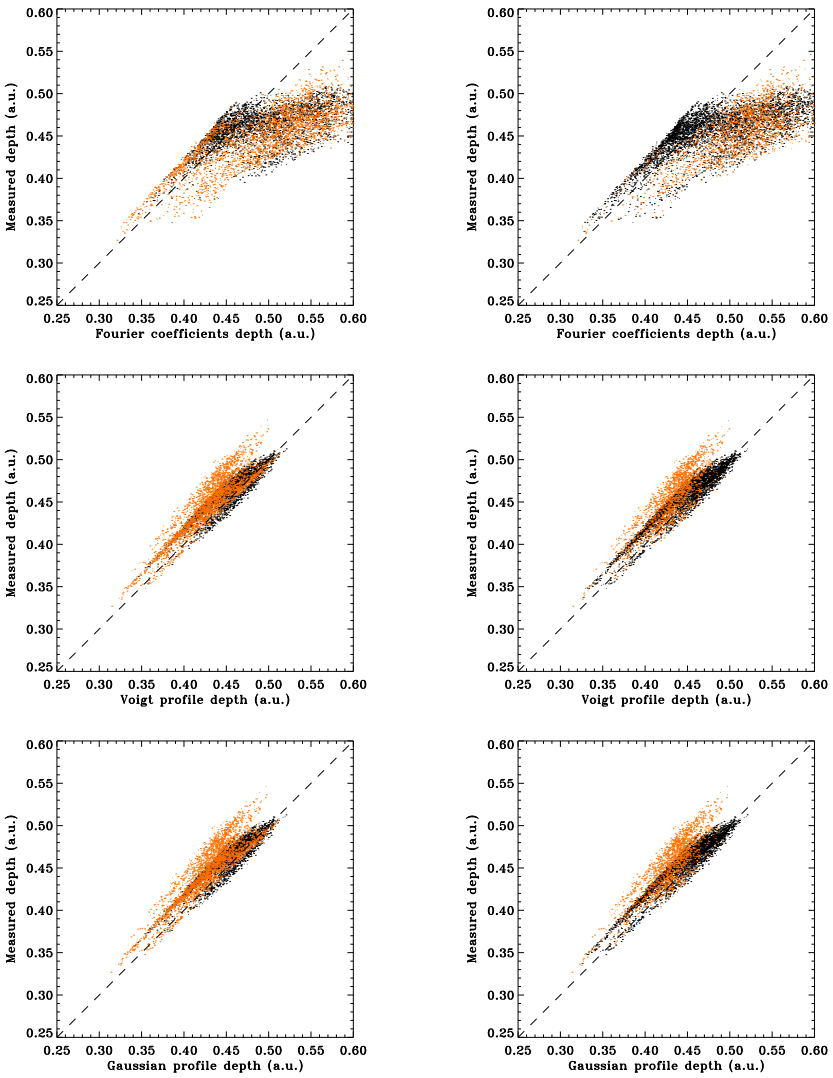


**Figure 11.** Scatter plots of the linedepth returned by different algorithms with the actual (measured) linedepths. Upper panels: MDI-like algorithm; middle panels: least-squares fit with a Voigt profile; lower panels: least-squares fit with a Gaussian profile. Left panels: the black dots show pixels for which the magnetic field inclination is larger than 57°, while the orange dots are for less inclined fields; right panels: the black dots show pixels for which the magnetic field strength is $< 1250$ G, while orange dots are for stronger fields.

MDI-like algorithm fares especially poorly in the sunspot, probably due to the significant deformation of the I+V and I-V Stokes profiles in strong and inclined magnetic fields. A (complicated) way to improve the MDI-like algorithms would be to implement different look-up tables, depending on how a reference model of the Fe I line varies with magnetic field strength and inclination, and use different look-up tables when a strong magnetic field is detected. It is proba-

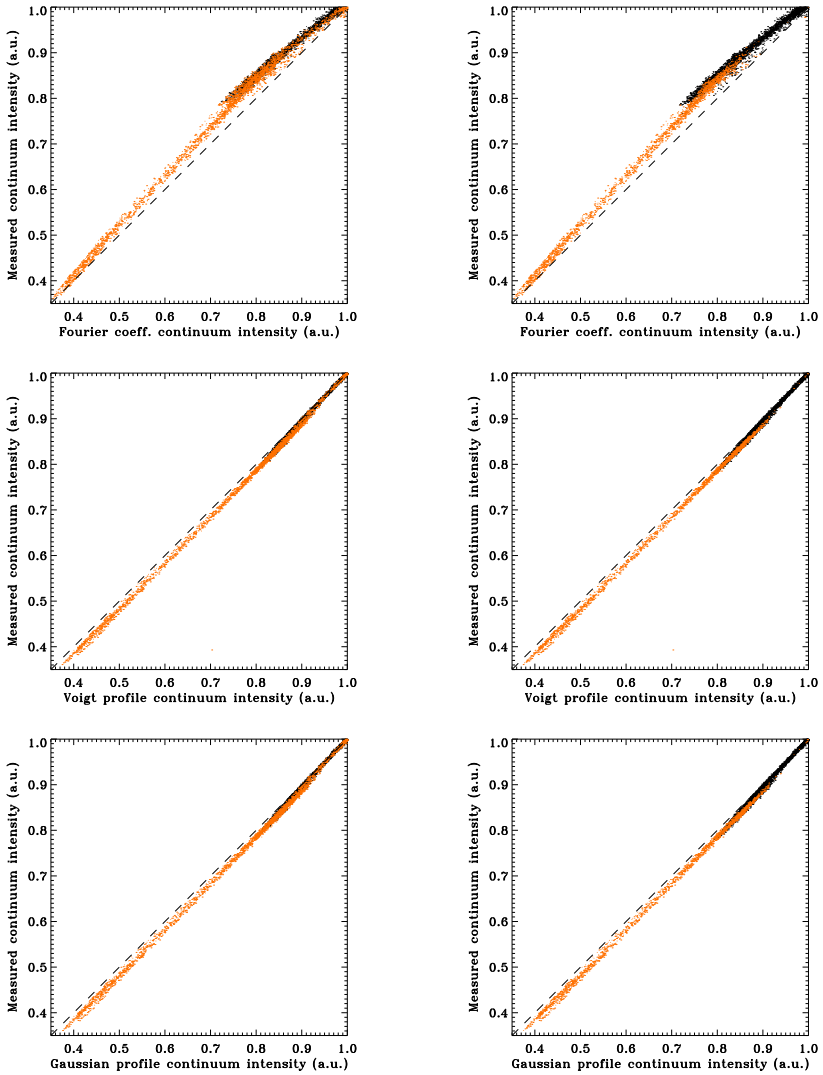


**Figure 12.** Scatter plots of the (normalized) continuum intensities returned by different algorithms with the actual (measured) continuum intensities. Upper panels: MDI-like algorithm; middle panels: least-squares fit with a Voigt profile; lower panels: least-squares fit with a Gaussian profile. Left panels: the black dots show pixels for which the magnetic field inclination is larger than 57°, while the orange dots are for less inclined fields; right panels: the black dots show pixels for which the magnetic field strength is $< 1250$ G, while orange dots are for stronger fields.

bly better to just abandon the MDI-like algorithm in favor of a least-squares fit. The main issue is the speed of the algorithm: least-squares fits are orders of magnitude slower than the MDI-like algorithm. The idea of combining 1st and 2nd Fourier-coefficient MDI-like results for Doppler velocity and LOS field strength is appealing in the quiet Sun to reduce the noise level due to photon noise, but will likely degrade the accuracy of the LOS observables in strong magnetic fields: the 2nd Fourier-coefficient MDI-like algorithm is unreliable in sunspots. Overall, despite its reduced accuracy compared to least-squares fit, the 1st Fourier-coefficients algorithm is actually performing relatively well even in presence of magnetic field. Using the results of this article it might be possible to partly correct the LOS observables derived by this algorithm as a function of the LOS magnetic field strength calculated. Since the IBIS data used here were taken prior to the launch of SDO, it would also be interesting to have simultaneous observations by HMI and IBIS, and to this end a proposal will shortly be submitted to the NSO. Finally, it should be reminded that the Fe I line seen by IBIS is slightly different from the HMI one (different PSFs for instance), and the lines used here have been convolved by the IBIS filter transmittances: therefore, the results obtained might be slightly different from what we would get from the actual HMI line profile.

**Acknowledgements** This work was supported by NASA Grant NAS5-02139 (HMI). We thank the HMI team members for their hard work. We also thank professor R. Ulrich for providing us with Fe I line profiles from Mount Wilson observatory.

## References

Bell, B., Meltzer, A.: 1959, *Smithsonian Contribution to Astrophysics* **3**, 39.
Borrero, J.M., Tomczyk, S., Kubo, M., Socas-Navarro, H., Schou, J., Couvidat, S., Bogart, R.: 2010, *Solar Phys.* in press.
Cavallini, F.: 2006, *Solar Phys.* **236**, 415.
Couvidat, S., Schou, J., Shine, R.A., Bush, R.I., Miles, J.W., Scherrer, P.H., Rairden, R.L.: 2011, *Solar Phys.* in press.
Dravins, D., Lindegren, L., Nordlund, Å.: 1981, *Astron. Astrophys.* **96**, 345.
Norton, A.A., Graham, J.P., Ulrich, R.K., Schou, J., Tomczyk, S., Liu, Y., Lites, B.W., Ariste, A. Lopez, Bush, R.I., Socas-Navarro, H., Scherrer, P.H.: 2006, *Solar Phys.* **239**, 69.
Rajaguru, S.P., Wachter, R., Sankarasubramanian, K., Couvidat, S.: 2010, *ApJ* **721**, L86.
Scherrer, P.H., Bogart, R.S., Bush, R.I., Hoeksema, J.T., Kosovichev, A.G., Schou, J., *et al.*: 1995, *Solar Phys.* **162**, 129.
Schou, J., Scherrer, P.H., Bush, R.I., Wachter, R., Couvidat, S., Rabello-Soares, M.C., *et al.*: 2011, *Solar Phys.* submitted.
Skumanich, A., Lites, B.W.: 1987, *ApJ* **322**, 473.
Tepper Garcia, T.: 2006, *MNRAS* **369**, 2025.
Wachter, R., Schou, J., Rabello-Soares, M.C., Miles, J.W., Duvall, T.L., Jr., Bush, R. I.: 2011, *Solar Phys.* in press.